

10. Burgoyne, L. N., Flynn, S. O. and Boylan, G. B., Undergraduate medical research: the student perspective. *Med. Educ. Online*, 2010, **15**; doi:10.3402/meo.v15i0.5212.
11. Houlden, R. L., Raja, J. B., Collier, C. P., Clark, A. F. and Waugh, J. M., Medical students' perceptions of an undergraduate research elective. *Med. Teach.*, 2004, **26**(7), 659–661; doi:10.1080/01421590400019542.
12. Oliveira, C. C., De Souza, R. C., Sasaki Abe, E. H., Silva Maz, L. E., de Carvalho, L. R. and Domingues, M. A. C., Undergraduate research in medical education: a descriptive study of students' views. *BMC Med. Educ.*, 2013, **14**(51), 5–8; <http://www.biomedcentral.com/1472-6920/14/51>.
13. Khan, H., Khawaja, M. R., Waheed, A., Rauf, M. A. and Fatmi, Z., Knowledge and attitudes about health research amongst a group of Pakistani medical students. *BMC Med. Educ.*, 2006, **6**, 54; doi:10.1186/1472-6920-6-54.
14. Al-Hilali, S. M., Al-Khatani, E. A., Zaman, B., Khandekar, R., Al-Shahri, A. and Edward, D. P., Attitudes of Saudi Arabia undergraduate medical students towards health research. *Sultan Qaboos Univ. Med. J.*, 2016; doi:10.18295/SQUMJ.2016.16.01.012.
15. Silcox, L. C., Ashbury, T. L., Van DenKerkhof, E. G. and Milne, B., Residents' and program director's attitudes toward research during anesthesiology training: a Canadian perspective. *Anesth. Analg.*, 2006, **102**, 859–864.
16. McKinnon, G., But I just want to be a good clinician, research in Canadian surgical training programs. *Ann. R. Coll. Physicians Surg. Can.*, 2002, **35**, 203–206.
17. Unnikrishanan, B. *et al.*, Medical students' research – facilitators and barriers. *J. Clin. Diagn. Res.*, 2014, **8**(12), XD01–XC04.

Received 9 October 2016; revised accepted 11 April 2017

doi: 10.18520/cs/v113/i06/1129-1134

Dual polarization lidar for remote sensing of aerosols and clouds in the atmosphere

Ajay Kumar Patel¹,
Bhavani Kumar Yellapragada^{1,*}, R. Vishnu²,
M. V. R. Murti¹ and James Jebaseelan Samuel³

¹Centre of Studies in Resources Engineering,
Indian Institute of Technology-Bombay, Powai, Mumbai 400 076, India

²National Atmospheric Research Laboratory,
Department of Space, Government of India, Gadanki 517 112, India

³Photonics, Nuclear and Medical Physics Division, VIT University,
Vellore 632 014, India

We describe an indigenously developed dual polarization lidar (DPL) system for remote sensing of the range-resolved properties of non-spherical nature of airborne and cloud particles. The DPL system probes the atmosphere using a linearly polarized second harmonic Nd:YAG laser. The design of receiver optics is such that it separates the collected backscattered light into

parallel and perpendicular polarization components. The ratio of intensity of perpendicular to parallel signals is known as the depolarization ratio (DR), which is a gauge for non-spherical particle content in the atmosphere. The DPL employs an external irradiance standard to calibrate the depolarization measurements. Comparison of simultaneous measurements between DPL and a similar instrument validates the utility of the system for cloud and aerosol studies. The altitude profiles of DR derived from lidar signals potentially indicate the type of major particle layers in the atmosphere.

Keywords: Aerosols, clouds, laser, polarization lidar, remote sensing.

ATMOSPHERIC aerosols, clouds and water vapour play a crucial role in climate change. The altitude of suspended aerosols in the atmosphere is an important issue for human health as well as the global environment. At lower altitudes aerosol particles are washed out from the atmosphere due to rain, and will not have a long-term effect on the climate. In the upper altitudes, aerosol particles are injected into the atmosphere from desert storms and biomass burning, and are frequently transported for more than thousands of kilometres and affecting remote areas¹.

The climate effects of atmospheric aerosols and clouds remain highly uncertain because of the lack of detailed data for the optical properties as well as the scarcity of information about the vertical distribution and spatial homogeneity of the particle layers. In addition to the optical properties, altitude information on particle non-sphericity is a vital parameter to understand aerosol and cloud microphysics. The particle shape critically controls its optical properties², and hence affects the earth's radiative process³ as well as the vertical distribution of the particles⁴.

Since the depolarization ratio (DR) is a measure of non-sphericity of the particles, it can also be considered as an indicator of the particle phase. Liquid droplet particles are mostly spherical in nature and indicate near-zero or low depolarization values, whereas solid crystals are non-spherical and indicate values substantially larger than zero. Moreover, hygroscopic nature of aerosol particles significantly affects the direct radiative forcing⁵. Hygroscopic particles contain water-soluble compounds and can change the shape of aerosol particles. Hence, the simultaneous altitude information of water vapour is essential to understand the hygroscopic behaviour of aerosol particles.

Recently, a cost-effective polarization-sensitive lidar was successfully developed and demonstrated for atmospheric studies at the National Atmospheric Research Laboratory (NARL), a unit of the Government of India under the Department of Space, located at Gadanki (13.5°N, 79.2°E, ~375 m above ground level (agl)) near Tirupati, Andhra Pradesh. Preliminary measurements of

*For correspondence. (e-mail: ypbk@narl.gov.in)

DR of high-altitude clouds and lower atmospheric aerosols have been broadly verified by Bhavani Kumar⁶. In this communication, we present the utility of an indigenously developed dual polarization lidar (DPL) for scientific studies using suitable comparisons. Table 1 gives the technical specifications of the DPL system. More details about the optical layout of DPL and its fabrication are given in Bhavani Kumar⁶.

Generally lidars are optimized to measure low light signal intensities using the single-photon counting technique. However, at strong light signal levels, this approach results in a nonlinear signal response. In the real atmosphere, due to the presence of a large amount of aerosol particles at lower heights, application of the photon counting method of detection undergoes a nonlinear process and fails to produce the true atmospheric response. In order to overcome the turbid characteristics of atmospheric boundary layer, the analog measurement of photomultiplier current is necessary in addition to photon counting signal detection. Due to this reason, the DPL receiver subsystem employs a two-channel transient recorder (TR) as the data acquisition unit. Each channel of the TR unit contains modules of analog and photon counting electronics. Each TR channel works with one optical detector and provides signals simultaneously both in analog and photon counting modes. Figure 1 *a* shows the individual signal profiles collected using analog and photon counting modes. The signal profiles shown in the figure correspond to the parallel polarized signal outputs of the DPL system. A combination of both signals gives the high linearity of the analog signal for strong signals and the high sensitivity of photon counting for weak optical signals. The integration of both detection mechanisms into a single profile is known as gluing. The main purpose of signal combination is that there is a region in the atmosphere where both signals are valid and have a high signal-to-noise ratio. After gluing the analog and photon count data, one gets a combined profile representing the extended photon count data (Figure 1 *b*). The method of gluing allows one to get photon count profile right from

the surface to about 30 km in 1 min time integration at 30 m range resolution. This gluing process has to be conducted before analysis of the DPL data for atmospheric studies. However, the application of gluing process is limited to clear sky observations only because the occurrence of low-level clouds influences photon counting detection. At the NARL site, the DPL system is generally operated with 1 min time integration at 30 m range bin setting. The lidar backscatter is generated by atmospheric targets such as molecules, aerosol and clouds, and the intensity of signal received depends on the attenuation of laser propagation through the atmosphere. The functional expression that relates outgoing laser energy (E_0) and the backscattered signal $P(z)$ is given as⁷

$$P(z) = KE_0 O(z) \frac{\beta_T(z)}{z^2} T^2(z) + P_b, \quad (1)$$

where E_0 is the transmitted laser pulse energy, K the lidar system constant and $O(z)$ is the overlap function (for dual polarization lidar system, $O(z) = 1$ for heights more than 340 m agl). $\beta_T(z)$ represents the total volume backscatter coefficient, which is the sum of backscatter from air molecules $\beta_m(z)$ and particles $\beta_a(z)$ received from the atmosphere. $T(z)$ refers to the atmospheric transmittance to the laser photons travelling from the ground to a given distance z in the atmosphere and back to the source. P_b indicates the sky background noise which corrupts the measured signal. For any lidar system, eq. (1) can be modified as

$$X(z) = (P(z) - P_b) z^2 = C \beta_T(z) T^2(z), \quad (2)$$

where $X(z)$ is a range-dependent quantity that is proportional to the attenuated backscatter. It is usually referred as the range-corrected backscatter and is computed after the processing of the background noise correction. The background noise represents a culminated photon quantity detected from light sources other than the radiated laser light, such as airglow emission, starlight and photo-detector dark counts. C is a proportionality constant that depends on system parameters.

One of the potential applications of lidar is to provide vital information on the altitude distribution of aerosols and clouds in the atmosphere. The advantage of the DPL system is that it can provide continuous measurements of the atmosphere during day and night without pause. During daylight period, the DPL provides important information on the growth of mixed layer and pollutant transport. During the nocturnal periods, the lidar has been successfully used to measure the scattering and depolarization characteristics of climatically important ice clouds in the upper troposphere, the mixed ice and supercooled water phase clouds at mid-levels, and the long-range-transported dust clouds with good height and temporal resolution. The line diagrams plotted in Figure 2 represent

Table 1. Major specifications of dual polarizatoion Lidar

Laser	Nd : YAG
Wavelength	532 nm
Laser pulse energy	30 mJ
Repetition rate	≤20 Hz
Beam-divergence	0.7 mrad
Telescope	Schmidt–Cassegrain
Pulse duration	5 ns
Field of view	Variable from 0.5 to 12 mrad
Data acquisition	Analog and photon counting
No. of receivers	2
Polarization diversity	0.1% accuracy
Vertical resolution	7.5 m max, 30 m typical
Range	Beyond 30 km, during night-time
Size	0.7 m ³
Operation	Zenith or at any slant path direction

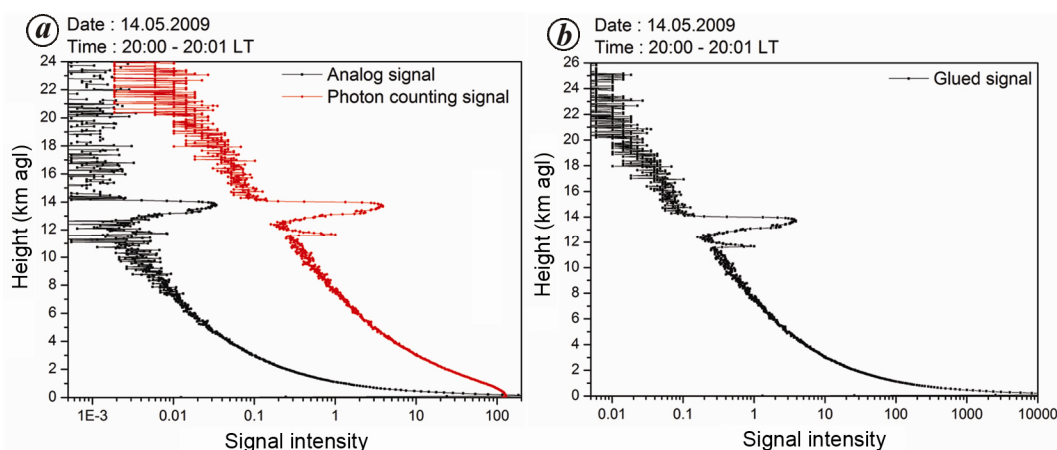


Figure 1. *a*, Range-resolved analog and photon counting signals obtained using DPL system representing the lidar parallel polarized channel outputs. The signals were acquired with a time and range resolutions of 1 min and 30 m respectively. *b*, A combined signal known as glued signal that obtained using a combination of analog and photon counting signals shown in (*a*). The glued signal extends the range of the photon counting signal in the lower atmosphere that enhances the dynamic range of the photon counting signal.

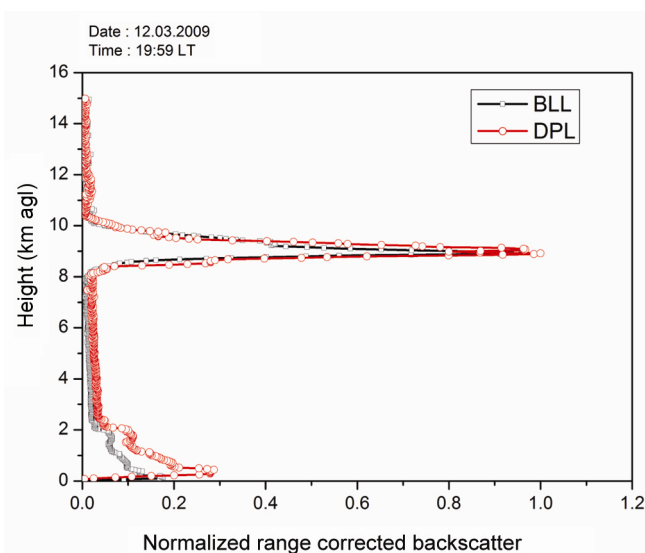


Figure 2. Altitude profiles of range-corrected backscatter representing two different lidar outputs, namely BLL and DPL. These lidars were operated simultaneously on 12 March 2009 during the passage of a high-altitude cloud over the NARL site. The range-corrected backscatter derived from the lidars was normalized to its peak to show the intensity variations.

the altitude distribution of range-corrected backscatter derived using data from two different lidars operated at the NARL site on 12 March 2009. It shows a simultaneous comparison of cloud and aerosol layers detection using the DPL and a similar lidar system⁸. The other lidar employed for comparison uses ISRO’s patent boundary layer lidar (BLL) technique⁶ which utilizes photon counting detection. It is a portable lidar that uses the second harmonic Nd : YAG laser for probing the atmosphere. We plotted a height–time–intensity (HTI) map using the simultaneous atmospheric data collected using the DPL and BLL systems on 12 March 2009 at the NARL site.

Figure 3 shows the HTI plot which is a continuous 10 h comparison between the DPL and BLL systems during the passage of a high-altitude cloud layer much above the local aerosol layer over Gadanki. This comparison shows the utility of the DPL system for the study of cloud and aerosol layers in the atmosphere.

We constructed the DPL system with a biaxial design between the transmitter and receiver units. We employed a linearly polarized pulsed Nd : YAG laser for probing the atmosphere. It operates at the second harmonic of the Nd : YAG laser. We employed 150 mm diameter telescope optics for collecting the laser backscatter at the defined field of view (FOV). We subsequently utilized a high-quality polarization beam-splitter in the receiver optics to separate the collected light into parallel and perpendicular polarized signal components. The signal polarization notions indicated here are with respect to the plane of polarization of the transmitter laser. DR is defined as the ratio of the backscatter cross-section in perpendicular polarization to the backscatter cross-section in parallel direction. DR is also equivalent to the ratio of the backscattered signals $P(z)$ measured in both polarization channels, multiplied by a calibration constant k

$$\delta(z) = \frac{\beta_{\text{perpendicular}}(z)}{\beta_{\text{parallel}}(z)} = k \frac{P_{\text{perpendicular}}(z)}{P_{\text{parallel}}(z)} \quad (3)$$

The atmospheric scatterers such as water droplets, which are homogeneous spheres (in terms of refractive index), produce the same state of polarization in the backscatter which is identical to the incident light. Hence, DR stays near zero as there is no change in the polarization state of return light⁹. However, for scatterers like aspherical/asymmetric particles, such as ice particles in clouds, the backscattered polarization state changes, which results

in a non-zero DR. The validity of DR measurements depends on the accuracy of the constant k . To estimate k , we performed lidar calibration using an external light source. For this, we employed a broadband light source whose irradiance spectral characteristics are traceable to the National Institute of Standards and Technology (NIST). We performed regular calibrations of the DPL system to maintain the accuracy of the measured DR values of aerosol and cloud layers. Moreover, we also conducted simultaneous DPL measurements whenever the CALIPSO satellite passed over the NARL site. However, the simultaneous observations were subject to clear sky conditions over the NARL site. The CALIPSO is a polar bound satellite that carries the CALIOP (Cloud Aerosol Lidar with Orthogonal Polarization), the first on-board lidar developed jointly by the US and France. The CALIOP is a two-wavelength lidar that has polarization measurement capability at 532 nm wavelength. The height profiles of depolarization derived from CALIOP provide information on remotely sensed details of

high-altitude cloud ice/water phase or thermodynamic phase¹⁰.

Figure 4 shows the altitude distribution of DR values measured using DPL when the CALIPSO satellite passed over NARL site on 28 April 2009. The DR values have been taken during the nearest transit period of the CALIPSO over NARL site, which is around 8 km away from Gadanki. The simultaneous comparison illustrates that the DPL-derived DR values are agreeing with the satellite lidar measurements. Higher values of DR indicate the presence of desert dust in the boundary layer¹¹. Several researchers reported the utility of polarization lidar for studies on long-range transport of desert dust^{12–14}. The long-range transported dust mixes with the other aerosols types in the boundary layer^{12,14} and produces local effects^{13,15}. The altitude variation of DR values indicate the identification of potential type of aerosol layers in the lower atmosphere, which are independent of aerosol load.

The unique application of polarization lidar lies in the identification of cloud phase of high-altitude clouds¹. Figure 5 presents the DPL observation of a mixed-phase

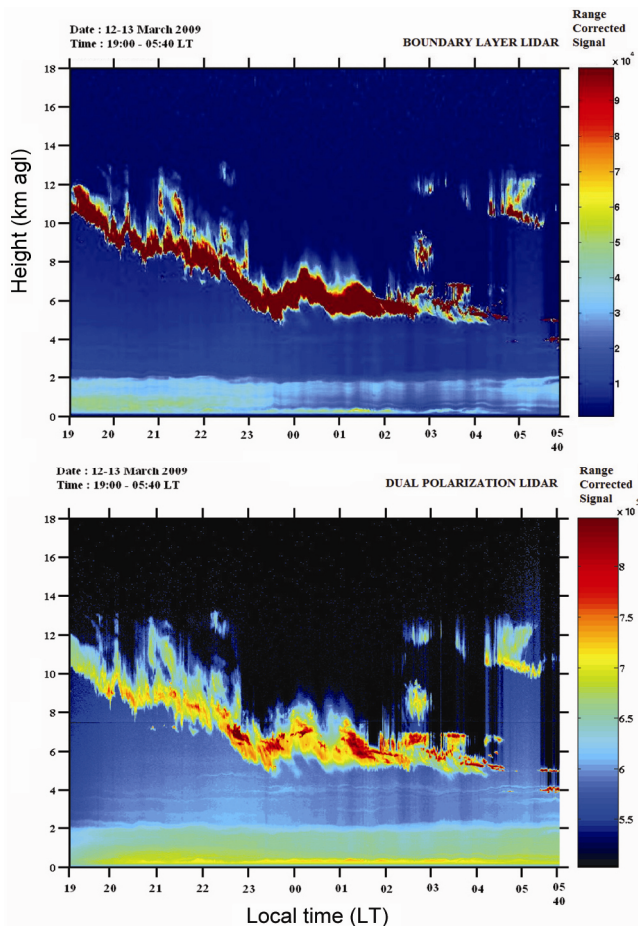


Figure 3. Simultaneous measurement of a high-altitude cloud using two different lidars that operated continuously from 12 March 2009 at 1900 LT till the early hours of the next day. The BLL and DPL signal profiles are presented in range-corrected backscatter. One can notice that both lidars detected a descending cloud layer much above the local aerosol layer which tops 2 km.

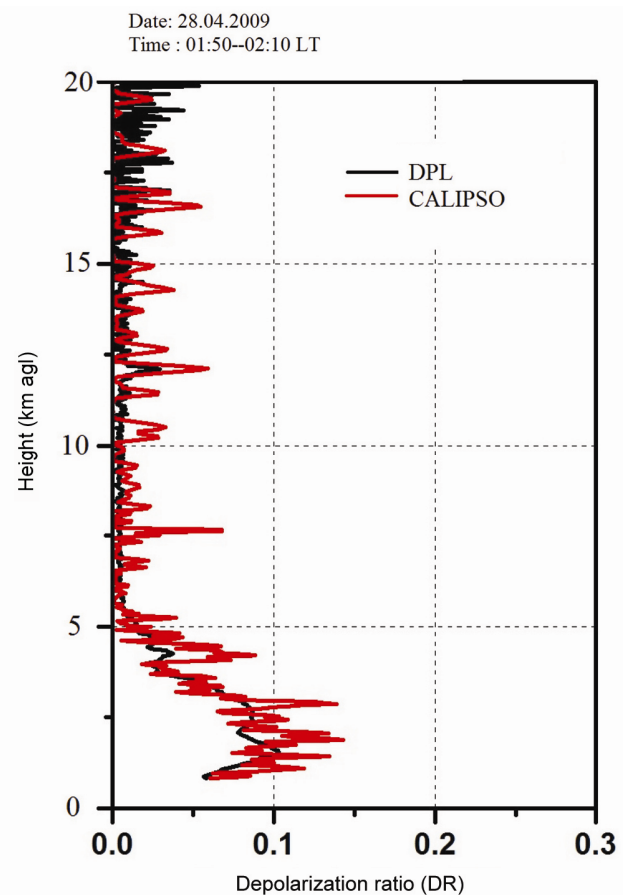


Figure 4. Simultaneous dust aerosol depolarization measurements over the NARL site using DPL and CALIPSO. The CALIPSO, measurements were taken during its pass close to the NARL site on 28 April 2009 at midnight hours.

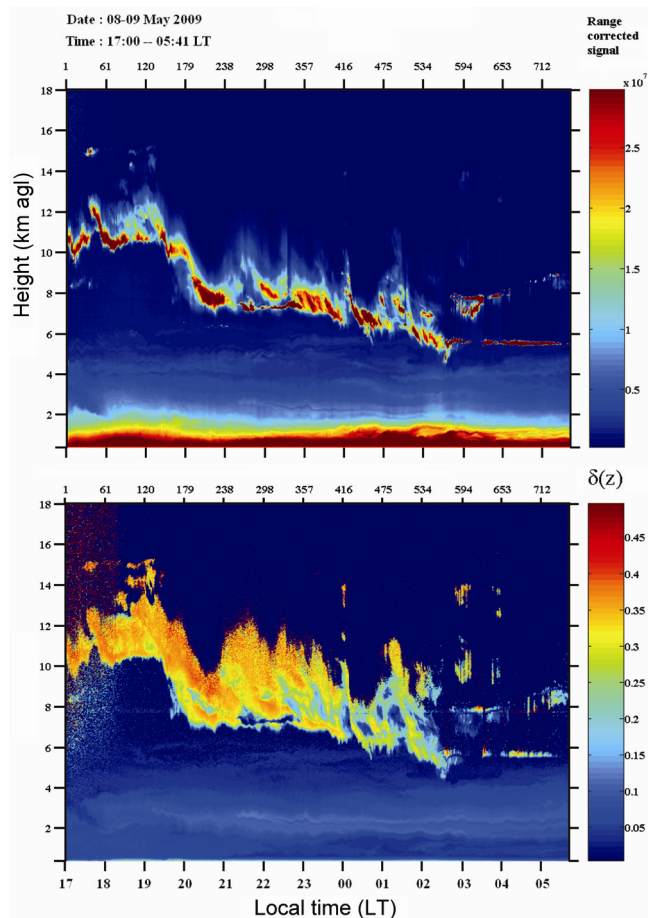


Figure 5. Time variation of range-corrected backscatter and depolarization ratio (DR) derived using DPL illustrating mixed phase cloud dynamics observed over Gadanki site on the night of 8 May 2009. One can notice significant change in the altitude structure of DR during its descent and dissipation.

cloud over the NARL site on 8 May 2009. The detected cloud is an altocumulus type that descended gradually and dissipated. Figure 5 shows both the DPL range-corrected backscatter and DR. The temporal variations of measurements presented in HTI form were obtained using DPL orientation in near-zenith condition. The altitude distribution of DR values within the cloud indicates that the observed cloud contains a mixture liquid water droplets and ice crystals coexist in a single layer. Precipitation of the ice particles that typically trail below super-cooled mixed-phase clouds, a phenomenon called virga, was clearly seen at the cloud base. The precipitating ice virga is associated with relatively high DR, and small lidar signal¹⁵. The liquid cloud base position can be identified by the start of strong backscatter and the corresponding near-zero depolarization δ that appeared in the observational period between 2100 and 2300 LT. Gradually the cloud layers descended while the altocumulus δ values decreased and the upper cirrus layers were again detected. An interesting observation is the evidence for elevated dust layers at lower heights. In this case, the lidar-

returned power display reveals that the aerosol scattering is barely discernible; so $\delta = 0.10$ – 0.15 represents a diluted mixture of dust with air¹⁴.

1. Sassen, K. and Benson, S., Ice nucleation in cirrus clouds: a model study of the homogeneous and heterogeneous mode. *Geophys. Res. Lett.*, 2005, **27**, 521–524.
2. Koepke, P. and Hess, M., Nonspherical particles and their influence on the scattering function of tropospheric aerosols. *J. Aerosol Sci.*, 1986, **17**(3), 254–257.
3. Lacis, A., Zhang, Y. C. and Rossow, W. B., Calculation of surface and top of atmosphere radiative fluxes from physical quantities based on ISCCP data sets 1. Method and sensitivity to input data uncertainties. *J. Geophys. Res.*, 1995, **100**, 1149–1165.
4. Liao, H. and Seinfeld, J. H., Radiative forcing by mineral dust aerosols: sensitivity to key variables. *J. Geophys. Res.*, 1998, **103**, 31637–31645.
5. Boucher, O. and Anderson, T. L. A., General circulation model assessment of the sensitivity of direct climate forcing by anthropogenic sulphate aerosols to aerosol size and chemistry. *J. Geophys. Res.*, 1995, **100**, 26117–26134.
6. Bhavani Kumar, Y., Lidar research activities and observations at NARL site, Gadanki, India. *Proc. SPIE*, 2016, **9879**, 98790S.
7. Collis, R. T. H., Lidar for routine meteorological observations. *Bull. Am. Meteorol. Soc.*, 1969, **50**, 688–694.
8. Bhavani Kumar, Y., Portable lidar system for atmospheric boundary layer measurements. *Opt. Eng.*, 2006, **45**(7), 076201.
9. Sassen, K. and Cho, B. S., Subvisual-thin cirrus lidar dataset for satellite verification and climatological research. *J. Appl. Meteorol.* 1992, **31**, 1275–1285.
10. Hunt, W. H., Winker, D. M., Vaughan, M. A., Powell, K. A., Lucker, P. L. and Weimer, C., CALIPSO Lidar description and performance assessment. *J. Atmos. Ocean. Technol.*, 2009, **26**, 1214–1228.
11. Murayama, T., Okamoto, H., Kaneyasu, N., Kamataki, H. and Miura, K., Application of lidar depolarization measurement in the atmospheric boundary layer: effects of dust and sea-salt particles. *J. Geophys. Res.*, 1999, **104**(D24), 31781–31792.
12. Sugimoto, N. *et al.*, Record heavy Asian dust in Beijing in 2002: observations and model analysis of recent events. *Geophys. Res. Lett.*, 2003, **30**(12), 1640; doi: 10.1029/2002GL016349.
13. Ansmann, A. *et al.*, Long range transport of Saharan dust to northern Europe: the 11–16 October 2001 outbreak observed with EARLINET. *J. Geophys. Res.*, 2003, **108**(D24), 4783, doi:10.1029/2003JD003757.
14. Shimizu, A. *et al.*, Continuous observations of Asian dust and other aerosols by polarization lidar in China and Japan during ACE-Asia. *J. Geophys. Res.*, 2004, **109**, D19S17; doi:10.1029/2002JD003253.
15. Sassen, K., The polarization lidar technique for cloud research: a review and current assessment. *Bull. Am. Meteorol. Soc.*, 1991, **72**, 1848–1866.

ACKNOWLEDGEMENTS. We thank the Atmospheric Science Programme Office of the Department of Space, Government of India for funding the lidar project at the National Atmospheric Research Laboratory (NARL), Gadanki. A.K.P. thanks the Indian Institute of Technology-Bombay for supporting the internship at NARL during his M Tech project.

Received 17 October 2016; revised accepted 18 April 2017

doi: 10.18520/cs/v113/i06/1134-1138